Water Research 183 (2020) 116074

Contents lists available at ScienceDirect

Water Research

journal homepage: www.elsevier.com/locate/watres

Kinetic modeling of the synergistic thermal and spectral actions on the inactivation of viruses in water by sunlight

Ángela García-Gil [a], Azahara Martínez [b], María Inmaculada Polo-López [b], Javier Marugán [a, *]

[a] Department of Chemical and Environmental Technology (ESCET), Universidad Rey Juan Carlos, C / Tulipán s/n, 28933, Móstoles, Madrid, Spain
[b] Plataforma Solar de Almería – CIEMAT, P.O. Box 22, 04200, Tabernas, Almería, Spain

ARTICLE INFO

Article history:
Received 25 February 2020
Received in revised form
5 June 2020
Accepted 15 June 2020
Available online 20 June 2020

Keywords:
Water temperature
Solar irradiance
Quantum yield
MS2 virus
SODIS
Household water treatment

ABSTRACT

Sunlight can be an effective tool for inactivating pathogens in water disinfection processes. In clear water, photoinactivation of viruses is driven by the absorption of UVB radiation and it is more efficient at shorter wavelengths. Moreover, the temperature can significantly improve the efficiency of the process. To date, no kinetic model has been reported that describes the simultaneous thermal and spectral effects that occur during the solar inactivation of viruses. This work presents a novel comprehensive kinetic model for the solar inactivation of MS2 coliphage as a function of the water temperature, irradiance, and spectral distribution of the incident radiation. The model is based on a combination of the modified Arrhenius equation, a wavelength-dependent first-order inactivation model with the quantum yield, and thermal parameters estimated from laboratory data. Model predictions have a 9% error with respect to experiments in the temperature range from 30 to 50 °C and UV irradiance range from 15 to 50 W/m^2. Moreover, the model was validated in three scenarios using different plastic materials that modify the spectral range of the radiation reaching the water, confirming an accurate prediction of inactivation rates for real solar disinfection systems worldwide using containers made of any material.

1. Introduction

Waterborne viruses are still a global challenge, especially for drinking water supply in low-income countries. The presence of viruses in drinking water sources is problematic due to their high resistance to disinfection processes compared to bacteria. Several factors have been found to influence the survival of viruses, being the most important: i) water characteristics, ii) water temperature, and iii) solar irradiance (Davies-Colley et al., 2000; Fisher et al., 2012, 2008; Gómez-Couso et al., 2010; Maynard et al., 1999; McGuigan et al., 2012; Sinton et al., 2002). The disinfection of water by exposure to sunlight is called SODIS process and it has been considered as a potential household water treatment for low-income countries. During solar exposure, water temperature can significantly increase above 30–40 °C with an observed synergistic effect between solar irradiation and water temperature (Castro-Alférez et al., 2017, 2018; Fisher et al., 2008; Gómez-Couso et al., 2010; McGuigan et al., 1998; Romero et al., 2011).

Solar inactivation of microbial pathogens can take place through three types of damaging mechanisms: i) direct endogenous damage, ii) indirect endogenous damage, and iii) indirect exogenous damage (Nelson et al., 2018). Endogenous damage (i and ii) is based on intracellular processes. While the direct damage (i) is caused by absorption of radiation by some of the microorganism constituents, indirect damage (ii) is the result of attacks to the microbial components by photo-produced reactive intermediates (PPRI) such as hydroxyl, carbonate and superoxide radicals, singlet oxygen carbonate radical or triplet state organic matter, which have been generated by sensitizers activated by solar photons (Nelson et al., 2018). In the case of the viruses, due to their simple structure consisting of a genome surrounded by a protein capsid, this indirect endogenous damage mechanism can be neglected. Finally, the indirect exogenous damage (iii) is based on the harmful effects of the external PPRI generated by external sensitizers present in unclear water. Therefore, photoinactivation of viruses in clear water can be reasonably assumed to take place mainly through direct endogenous damage based on the absorption of UV-B solar radiation (Love et al., 2010).

* Corresponding author.
E-mail address: javier.marugan@urjc.es (J. Marugán).

https://doi.org/10.1016/j.watres.2020.116074

Viruses have been demonstrated to be very sensitive to wavelengths from 280 to 320 nm and, in general, the shorter the wavelength, the more harmful the damage. The action spectra of photoinactivation closely keep the shape of the absorption spectra of the nucleic acids and proteins (Lytle and Sagripanti, 2005). One example of this is coliphage MS2, a single-stranded RNA virus that infects *Escherichia coli* bacteria and other Enterobacteriaceae, which is commonly used as an indicator of photoinactivation due to its higher resistance in comparison with other viruses or bacteria (Love et al., 2010; Theitler et al., 2012). In this regard, the selection of the material employed for the manufacturing of the solar disinfection systems (in particular its transmittance in the UV-B range) is a critical factor for the efficacy of the process (García-Gil et al., 2020a).

In the literature, many efforts have been made to develop kinetic models of the inactivation using biological weighting functions considering the spectral sensitivity of MS2. Fisher et al. (2011) pioneered the measurement of the action spectra for MS2, fitting wavelength-dependent experimental results with a constrained nonlinear multivariable optimization function. Mattle et al. (2015a) calculated the inactivation as a function of the rate of photon absorption by the virus (the result of the extinction coefficient by irradiance for each wavelength) and the quantum yield, keeping the biological fundamentals of the mechanism. Silverman et al. (2019) concluded that the best kinetic model was that of Mattle et al. (2015a) with a new quantum yield optimized within a larger batch of experiments. As yet, however, no model has taken into account the combined thermal-photonic synergistic effect with the action spectra for the coliphage MS2 solar inactivation. This work presents a novel approach for the kinetic modeling of the thermal and wavelength-dependent solar inactivation of the MS2 virus. The predictions of the model have been successfully validated with experimental data from solar water disinfection using materials of different spectral transmission.

2. Material and methods

2.1. Chemicals and organisms

MS2 coliphage (ATCC 15597B1) and the bacterial host *E. coli* C300 171 (ATCC 15597) were used in the experiments. Aliquots of virus stock solution were added directly into the vessel with the water matrix to provide an initial concentration of 10^5-10^6 Plaque Forming Units (PFU)·mL^{-1}. Stocks of MS2 infective particles and enumeration were prepared using Tryptone Yeast Glucose (TYG) medium containing the following reagents from Sigma-Aldrich: Tryptone (10.0 g L^{-1}) Yeast Extract (1.0 g L^{-1}), NaCl (8.0 g L^{-1}), Glucose (10.0 g L^{-1}), $CaCl_2$ (2.94 g L^{-1}) and Thiamine (0.01 g L^{-1}); additionally, 5 and 15 g L^{-1} of Bacteriological Agar was added to prepare semi-solid and solid agar medium, respectively. The *E. coli* host was cultivated for 6 h in fresh liquid medium (TYG) at 37 °C with a rotatory agitation of 90 rpm previously to MS2 enumeration. The enumeration of infective MS2 was determined by a double-layer agar method. Briefly, 1 mL of *E. coli* C300 was mixed with 0.1–0.5 mL of sample (or 10-fold dilutions using Phosphate Buffer Saline) and 5 mL of melted semi-solid TYG agar. The mix was then poured on solid TYG agar Petri dishes. Solidified plates were incubated upside-down at 37 °C for 24 h. The detection limit of this method was 2 PFU mL^{-1}.

2.2. Experimental design

Three sets of experiments were conducted. Firstly, experiments were carried out at different water temperatures (30, 40, 45, and 50 °C) under dark conditions in order to estimate the contribution of the water temperature effect in the dark thermal inactivation of MS2 virus. Secondly, inactivation experiments were carried out under different UV (280–400 nm) irradiances (15, 20, 30, 40, and 50 W m^{-2}) and water temperatures (30, 40, 45, and 50 °C) to calibrate the irradiance effect and its synergistic effect with water temperature. As a reference, the UV (280–400 nm) irradiance of the ASTM G173 a.m. 1.5 standard solar spectrum is 46.1 W m^{-2}. Finally, experiments for the validation of the model predictions were carried out using plastic materials with different UV-B transmittance. Plastic sheets were placed between the radiation source and the water to assess the effect of the spectral distribution on the efficacy of the inactivation. The sheets materials comprised polyethylene terephthalate (PET), polypropylene (PP) and polymethylmethacrylate (PMMA). These plastics were selected due to the fact that they are potential materials for the manufacturing of SODIS containers (García-Gil et al., 2020a). For the three scenarios, experiments were conducted at 15 and 50 W m^{-2} of UV (280–400 nm) radiation and water temperatures of 30, 40, and 50 °C.

Inactivation of the MS2 virus was studied in autoclaved distilled water with sodium chloride (0.9% w/v) at an initial MS2 concentration of 10^5 PFU mL^{-1}. Experiments were carried out in a solar simulator (Atlas Suntest XLS+, USA) equipped with a xenon lamp and a combination of filters to simulate the outdoors solar radiation spectrum. The emission spectrum and the irradiance were measured with an AvaSpec-ULS2048 (200–800 nm). The reactor used for these experiments was an open glass vessel with a diameter of 19 cm and a total volume of 700 mL. The exterior of the vessel was completely black to avoid uncontrolled light reflections and guarantee that only the measured direct radiation participates in the process. Constant stirring of 250 rpm was kept during the experiments to ensure a homogeneous concentration of MS2 virus.

2.3. Kinetic modeling

The kinetic analysis of the experimental data was carried out through the estimation of the kinetic parameters for the different sub-models according to the following sequential steps: i) dark thermal inactivation, ii) global UV irradiance and thermal synergistic effect, iii) wavelength-dependent spectral action, and iv) spectral-thermal synergistic effect.

2.4. Dark thermal inactivation

No kinetic description was required for the dark inactivation since the experimental data recorded in the potential environmental temperature range (up to 50 °C) showed negligible inactivation results (Fig. S1).

2.5. UV irradiance and thermal synergistic effect

The inactivation data were fitted to a first-order kinetic model (Eq. (1)):

$$\frac{dC}{dt} = -k \cdot C \tag{1}$$

$$\ln\left(\frac{C}{C_0}\right) = -k \cdot t \tag{2}$$

where C_0 is the initial concentration of the MS2 virus (PFU·mL^{-1}), C is the concentration at a specific time t, and k is the kinetic constant. In the case of linear dependence on the inactivation with the irradiance, the kinetic constant would be explicitly proportional to the global UV (280–400 nm) irradiance (I) according to Eq. (3):

$$\ln\left(\frac{C}{C_0}\right) = -k' \cdot I \cdot t \quad (3)$$

Despite the negligible effect of temperature in the dark inactivation, a thermal-radiation synergistic effect was considered to describe the influence of temperature on the photoinactivation of MS2. A modified Arrhenius equation with a threshold temperature, was used to describe the effect of the water temperature (T) on the photoinactivation kinetic constant (k'):

$$k' = k_0\left(\frac{T}{T_0}\right)^n \cdot \exp\left(-\frac{E_a}{R}\cdot\left(\frac{1}{T}-\frac{1}{T_0}\right)\right) \quad (4)$$

where k_0 is the temperature-independent pre-exponential factor, n is a constant, E_a is the activation energy, R is the universal gas constant and T_0 is the threshold temperature. As Peleg et al. (2012) demonstrated, the threshold temperature can be omitted, leading to a different value of k_0 for the same value of k'. However, the present model kept the T_0 as a conceptual threshold to account for the limit temperature above which the synergistic effects are observed. The kinetic parameters of the model (k_0, n and E_a/R) have been calculated by minimizing the normalized root mean square error (NRMSE) between the predicted and observed kinetic constant in the experiments, using a constrained nonlinear multivariable optimization algorithm (Microsoft Excel solver).

2.6. Wavelength-dependent spectral action

The kinetic model proposed by Mattle et al. (2015a) was used for modeling the sunlight inactivation of MS2 considering a biological weighting function to describe the spectral action (Eqs. (5)–(7)). The inactivation rate can be expressed as:

$$\frac{dC}{dt} = -\varphi_V \cdot P^V \quad (5)$$

where φ_V is the quantum yield of virus inactivation (PFU·photon^{-1}) and P^V is the volumetric rate of photon absorption by the virus (photon·s^{-1}·mL^{-1}), calculated as:

$$P^V = \int_\lambda p^0(\lambda)\cdot\varepsilon_V(\lambda)\cdot C\cdot d\lambda \quad (6)$$

$p^0(\lambda)$ is the spectral photon flux density (photon·s^{-1}·m^2·nm^{-1}) that, in clear water and short optical pathway, can be assumed to be constant and equivalent to that in the inlet surface. $\varepsilon_V(\lambda)$ is the spectral extinction coefficient of the virus (mL·PFU^{-1}·cm^{-1}) whose values, in the range from 240 to 400 nm, can be obtained from the literature (Mattle et al., 2015a).

By combining Eq. (2) with Eq. (6), the kinetic constant of inactivation takes the form:

$$k = \varphi_V \cdot \int_\lambda \varepsilon_V(\lambda)\cdot I(\lambda)\cdot\frac{\lambda}{h\cdot c}\cdot d\lambda \quad (7)$$

where $\frac{\lambda}{h\cdot c}$ (photon·J^{-1}) converts the energy units of the spectral irradiance, $I(\lambda)$, to the photonic units of $p^0(\lambda)$, being h the Planck's constant and c the speed of light in vacuum.

The values of the quantum yield were calculated by minimizing the NRMSE between the predicted and observed kinetic constant of experimental data with negligible thermal synergy effects obtained by nonlinear optimization with Microsoft Excel solver.

2.7. Spectral-thermal synergistic effect

At this point, the first-order kinetic constant for the MS2 photoinactivation is defined by two different processes: i) kinetic constant as a function of water temperature and radiation (Eq. (4)), and ii) kinetic constant as a function of action spectra (Eq. (7)). In order to develop a model that involves both processes in a single expression, the quantum yield was defined as a function of water temperature (Eq. (8)):

$$\varphi_V = \varphi_V^0 \cdot \left(\frac{T}{T_0}\right)^n \cdot \exp\left(-\frac{E_a}{R}\cdot\left(\frac{1}{T}-\frac{1}{T_0}\right)\right) \quad (8)$$

where n, E_a/R and T_0 took the values previously calculated, and φ_V^0 was estimated by minimizing the NRMSE between the predicted and observed kinetic constant by nonlinear optimization.

3. Results and discussion

3.1. Dark thermal inactivation

Experiments under dark conditions were carried out at 30, 40, 45, and 50 °C in order to study the effect of water temperature on the MS2 inactivation (Fig. S1). In all cases, the reduction in the concentration of viable viruses is negligible and lower than the experimental error. Therefore, dark thermal inactivation alone can be discarded. This is in agreement with Romero et al. (2011), who found that direct photolysis was responsible for MS2 solar inactivation in the 14–42 °C temperature range in the absence of external sensitizers.

3.2. UV irradiance and thermal synergistic effect

Data from MS2 inactivation experiments under illuminated conditions (15, 20, 30, 40, and 50 W m^{-2}) at different water temperatures (30, 40, 45 and 50 °C) were fitted with Eq. (2) (first-order kinetic model). Table S1 shows the observed average values of the kinetic constant for the different experimental conditions, calculated from at least two replicates in all cases and with a fitting correlation factor higher than 0.99. An obvious relation between the values of the kinetic constant and the irradiance can be clearly observed (Fig. 1A): the higher the irradiance, the higher the value of k. This dependence is proved to be linear (as expressed in Eq. (3)) when plotting the values of the calculated kinetic constant (k, min^{-1}) divided by the irradiance (k', m^2·W^{-1}·min^{-1}) (Fig. 1B) and it shows that the values are similar for each temperature with differences in the range of the experimental error.

In contrast with the results of dark thermal inactivation (Fig. S1), Fig. 1 shows that water temperature clearly affects the photoinactivation rate at T > 40 °C. This synergistic effect has been included in the model by means of the temperature dependence of the kinetic constant according to the modified Arrhenius equation, using a value of 40 °C (313 K) for the temperature threshold (T_0). As shown in Fig. 1, this is the value above which the photoinactivation kinetics seems to be affected by temperature. In any case, the value of T_0 is arbitrary, leading to different values of k_0 and n for the same values of k (as shown by Peleg et. Al (2012)). Calculation of the kinetic parameters (n = 423, k_0 = 3.84 × 10^{-3} min^{-1} and $E_a/R = -1.30\cdot10^5$ K) was carried out by simultaneous fitting of the experimental data for the entire range of irradiances and temperatures with an NRMSE of 10.3% (see Fig. S2.1, S2.2, S2.3, and S2.4).

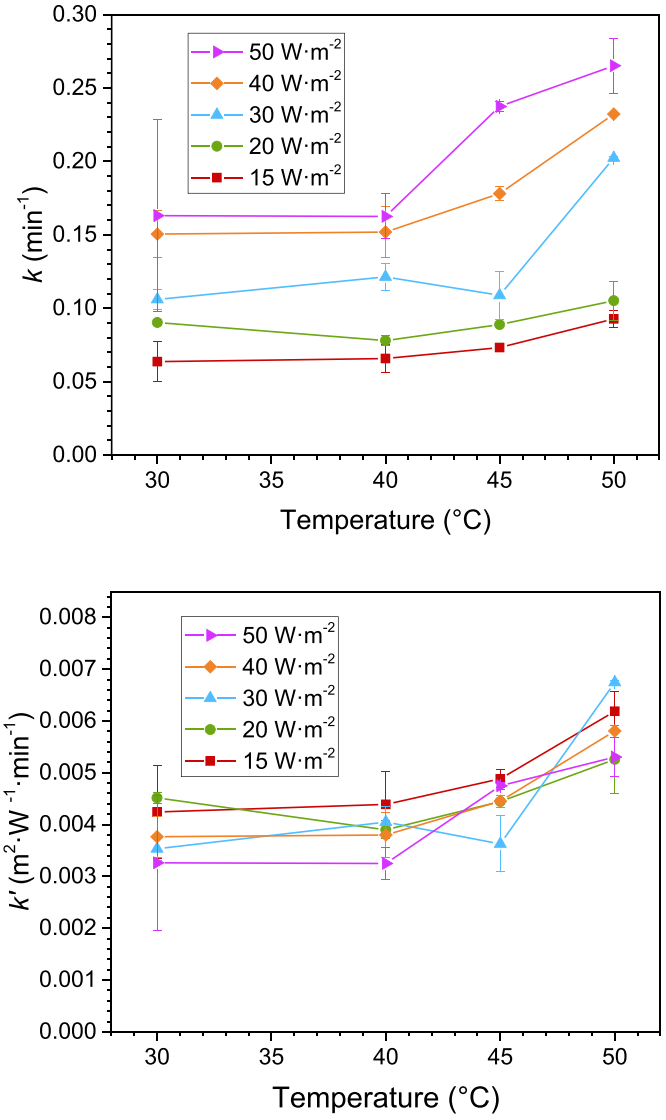

Fig. 1. Values of the first-order kinetic constant for experiments under different UV irradiance and water temperature. A) k (min^{-1}) (top). B) $k' = k / I$ ($m^2 \cdot W^{-1} \cdot min^{-1}$) (bottom). Error bars calculated from the standard deviation of replicate experiments.

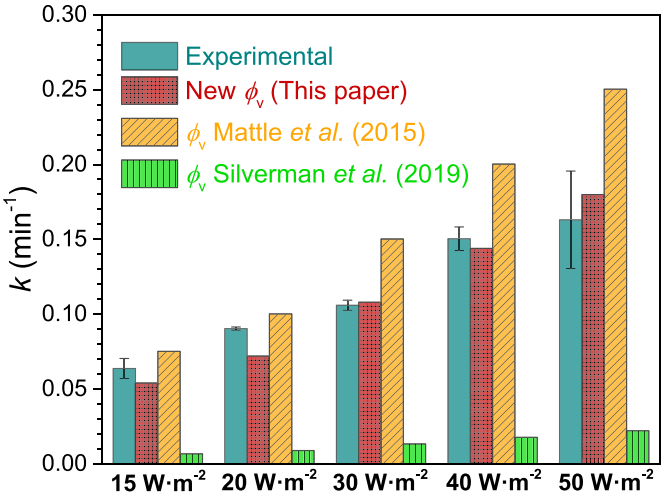

Fig. 2. Comparison of the observed MS2 photoinactivation kinetic constant and the prediction of action spectra models using different quantum yield values (φ_V) Error bars calculated from the standard deviation of replicate experiments.

3.3. Wavelength-dependent spectral action

The model developed so far satisfactorily reproduces the solar inactivation of MS2 virus as a combination of UV irradiance and thermal effects. However, this model can only be applied to water disinfection processes using radiation with the exact spectral distribution of the solar light. If the spectral distribution of the incident radiation is modified but the global UV remains the same, the effective damage can change dramatically. Therefore, the wavelength-dependent spectral action of the MS2 photoinactivation needs to be modeled in order to predict the behavior of solar disinfection containers with different transmission spectra. As suggested by Mattle et al. (2015a), the MS2 inactivation rate can be calculated by multiplying the quantum yield, the concentration of viruses, and the volumetric rate of photon absorption (calculated as the integration in wavelength of the spectral virus extinction coefficient by the spectral irradiance for each wavelength). MS2 virus extinction coefficients were taken from the literature (Mattle et al., 2015a), whereas the quantum yield was calculated from experimental data of the inactivation at 30 °C (in which thermal effects can be neglected, Fig. 1). Spectral data of the incident light from 280 nm (below which solar irradiance is negligible) to 400 nm (above which radiation absorption by MS2 virus can also be neglected) were used (see Table S3). The calculated quantum yield was $\varphi_V = 2.07 \cdot 10^{-3}$ PFU inactivated per absorbed photon with an error value of 11% (NRMSE). As a reference, the error values calculated between the observed MS2 photoinactivation kinetic constant and the prediction of action spectra models using the quantum yield values reported by Mattle et al. (2015a) and Silverman et al. (2019) were 43% and 92%, respectively (Fig. 2 and Table S2). Although the three models use the same type of biological weighting function based on the virus absorption spectra, the observed discrepancies are the result of different experimental sets and calculation procedures. The new quantum yield calculated in this work was found to be between the quantum yields calculated by other authors but closer to the one reported by Mattle et al. (2015a) that used the same spectral range from 280 to 400 nm for the calculation. In contrast, Silverman et al. (2019) considered irradiance data from 290 nm. Although the irradiance in the 280–300 nm range is very low, the sensitivity of the MS2 virus at these wavelengths is very high (which is reflected in the extinction coefficient). The reason for these apparent discrepancies is the high sensibility of the results to the experimental data provided by the spectroradiometer. Small variations of spectral irradiance in the range from 280 to 300 nm could lead to significant differences in the calculation of the global quantum yield.

3.4. Spectral-thermal synergistic effect

Finally, the complete model was developed by combining the radiation and thermal synergistic model with the action spectra previously described. In general, it is expected that, due to the thermal sensitivity of the virus demonstrated above, more viruses will be inactivated per absorbed photon if the water temperature is higher. Using the values of the thermal parameters calculated previously ($T_0 = 313$ K, $n = 423$ and $Ea/R = -1.3 \cdot 10^5$ K), the value of the pre-exponential quantum yield (φ_V^0 in Eq. (8)) was calculated from the simultaneous fitting of all the experimental data, i.e. $2.15 \cdot 10^{-3}$ PFU were inactivated per absorbed photon. The NRMSE fitting error was 9.2%, which is lower than the 10.3% found in the thermal synergistic model considering the total UV irradiance. This fact confirms the meaningful enhancement of the model when the

action spectrum is considered and the improved prediction capabilities of the complete model represented by the first-order kinetics constant calculated by Eq. (9):

$$k = \varphi_V^0 \left(\frac{T}{T_0}\right)^n \exp\left(-\frac{E_a}{R}\left(\frac{1}{T}-\frac{1}{T_0}\right)\right)\int_\lambda \varepsilon_V(\lambda) I(\lambda)\frac{\lambda}{hc}d\lambda \quad (9)$$

Predicted inactivation kinetic constants were compared to the observed values in Fig. 3 and showed a very good agreement with a random distribution of the fitting error. Moreover, when the values of the kinetic constants are divided by the irradiance, all the curves clearly overlap (Figure 1.B), as expected from the linear dependence of the reaction rate with the irradiance.

3.5. Validation of the model

The remarkable strength of the developed model is its capability of predicting the MS2 photoinactivation rate under different solar spectral irradiance and environmental temperature conditions for different locations worldwide. Moreover, for the specific application of solar water disinfection, the model allows accurate calculation of the expected inactivation rate as a function of the transmission spectra of the container. The validation of the model predictions was carried out using plastic materials of different UV-B transmittance (i.e. PET, PP, and PMMA). The transmission of the materials in the global UV-B range is 1%, 44%, and 57% and, in the UV-A range, 59%, 60%, and 86%, respectively. The radiation transmitted by the plastics for a global UV (280–400 nm) irradiance of 50 W m^{-2} and the extinction coefficients that describe the spectral sensibility of the MS2 virus to the photoinactivation are shown in Fig. 4 (see the data in Table S3). As can be observed, the UV-B is the critical region in which the virus absorption overlaps with the available incident radiation.

Fig. 5 shows the comparison between the observed and the predicted kinetic constants for PET, PP and PMMA scenarios. If we consider the fully predictive nature of the kinetic constants calculated by the model (they are not fitting values but predictions from the model using kinetic parameters calculated in a completely different experimental set of data), the agreement can be considered to be very good, with reasonable values of NRMSE of 28% and 18% for PP and PMMA, respectively. In the case of PET, the NRMSE is much higher (60%) due to the very low values of the inactivation rates achieved by this low UV-B transmission material. For the PP and PMMA scenarios, the observed inactivation rates were obviously lower than those without plastic due to their partial transmittance. However, despite the higher transmittance of the PMMA in the global UV-B range, the kinetic constants were higher in the PP scenario. The reason is that PP transmission is slightly higher in the 280–290 nm range, where the photons produce greater damage. However, as shown in Fig. 4, the emission of the solar simulator overestimates the irradiance of the standard AM 1.5 solar spectrum, especially in the 280–300 nm range where the process is especially sensitive. Consequently, under real sunlight, PP would be expected to perform similarly or even slightly worse than PMMA.

Model validation confirms the remarkable potential of the spectral-thermal synergistic model to predict MS2 photoinactivation with sunlight under different spectral and global irradiance values and temperatures around the world, specifically for the application of solar water disinfection processes with any kind of container. Moreover, the methodology and mathematical model presented can easily be extrapolated to other viruses and

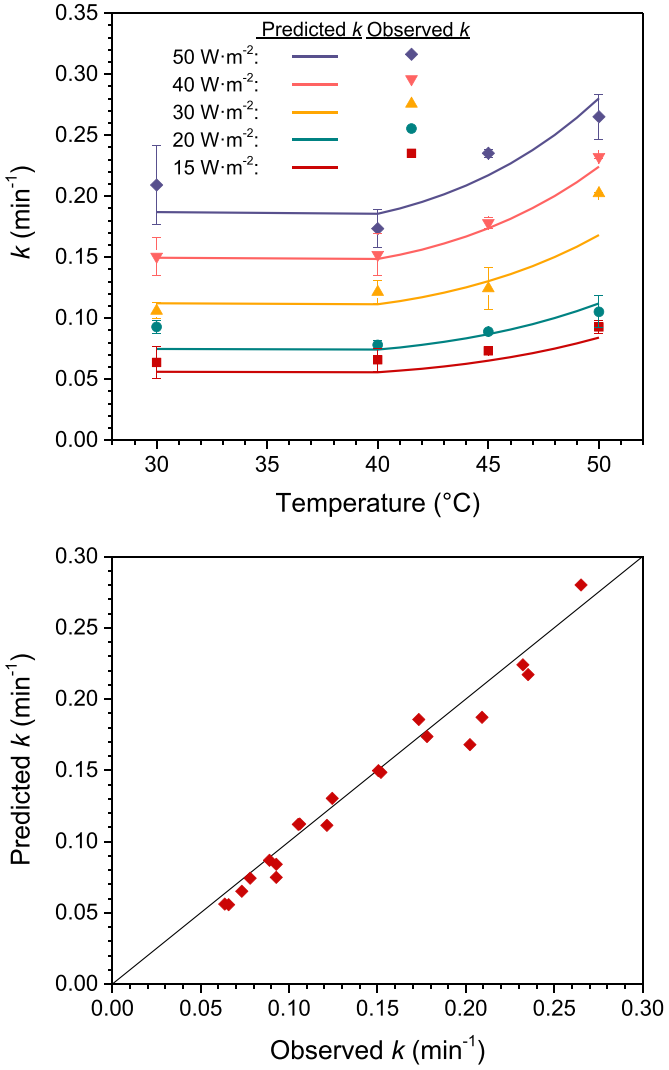

Fig. 3. Observed first-order kinetic constant for MS2 photoinactivation and predictions of the spectral-thermal synergistic model. Effect of temperature and irradiance (top) and agreement between observed and predicted kinetic constants (bottom). Error bars calculated from the standard deviation of replicate experiments.

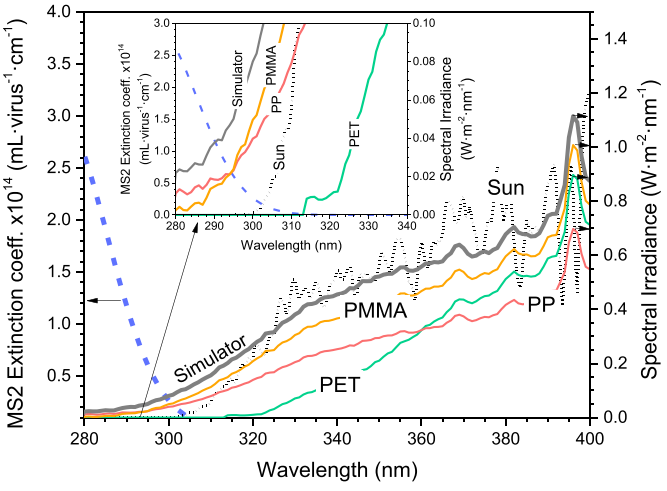

Fig. 4. Extinction coefficient of MS2 virus (Mattle et al., 2015a) (left axis) and spectral irradiance of the solar simulator and transmitted by PMMA, PP, and PET plastics (solid lines) and ASTM G-173 reference AM 1.5 solar spectrum (dot line) (right axis). Inset: Details of the UV-B region.

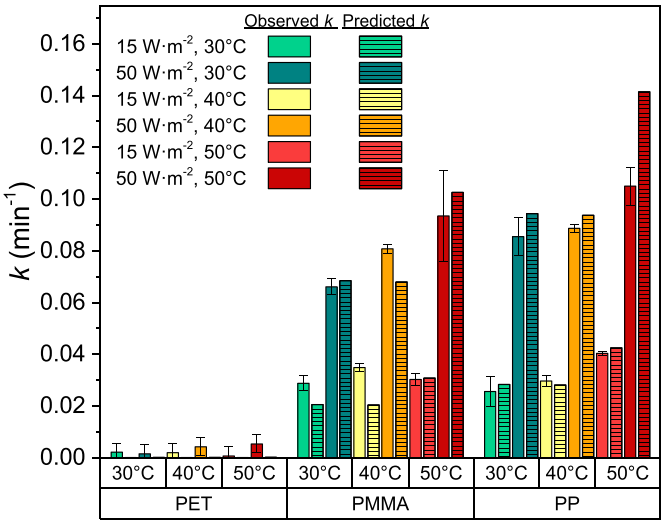

Fig. 5. Observed and predicted MS2 photoinactivation kinetic constant for experiments of validation using PP, PMMA, and PET to modify the spectral distribution of radiation. Predicted constants calculated with the spectral-thermal synergistic model. Error bars calculated from the standard deviation of replicate experiments.

pathogens with the obvious recalculation of the specific kinetic parameters.

However, this model has been developed for clear water and, in real conditions, water could contain naturally occurring substances that can act as external sensitizers (i.e. natural organica matter, NOM) and/or attenuating factors (i.e. turbidity). Several PPRI have been found to participate in the virus inactivation such as hydroxyl radicals (Mattle et al., 2015b), triplet state organic matter (Rosado-Lausell et al., 2013), carbonate radicals (Mattle et al., 2015b) and, especially, singlet oxygen (Kohn et al., 2007; Kohn and Nelson, 2007; Rosado-Lausell et al., 2013). Although most of these substances can be removed by a previous household filtration (using cloth or ceramic filters) or by the spontaneous decantation during SODIS process (WHO, 2002), if their presence in water cannot be neglected, they should be considered in the model to enhance the prediction of field conditions (Kohn et al., 2016). Furthermore, in the case of using high volume containers, the damage produced by the external PPRI can be completely overshadowed by the role of the sensitizers as attenuators of radiation (García-Gil et al., 2020).

4. Conclusions

A novel comprehensive kinetic model for the MS2 inactivation in clear water at ambient conditions has been developed as a function of the water temperature, irradiance and spectral response of the virus. The model predictions show a great agreement (average error of 9%) with experimental data obtained in a solar simulator.

The developed model considers for the first time the effect of water temperature on the virus inactivation, showing no effect in the dark, but a strong thermal-photonic synergy under solar illumination at temperatures above 40 °C.

Regarding the irradiance and the spectral distribution of the incident light, the model reproduces the expected biological spectral action according to the radiation absorption spectra of the viral DNA. Taking into account explicitly the spectrum of the light, the model can predict the MS2 inactivation rate at different locations around the world and using containers made of materials with different transmission spectra employed to disinfect water by the SODIS process at the household level. Model predictions were validated using PET, PP and PMMA materials, with errors of 28% and 18% for PP and PMMA, respectively, and insignificant inactivation for PET, the material most widely used for SODIS processes. In any case, application of the model to field conditions could require recalibration of the kinetic parameters to account for the specific substances present in the water that could either enhance the process acting as sensitizers for the generation of PPRI or to the contrary diminish the efficiency by their role as attenuators of radiation.

Declaration of competing interest

The authors declare that they have no known competing financial interests or personal relationships that could have appeared to influence the work reported in this paper.

Acknowledgments

The authors gratefully acknowledge the financial support of the European Union's Horizon 2020 research and innovation program under WATERSPOUTT H2020-Water-5c-2015 project (GA 688928). Ángela García Gil also acknowledges Técnicas Reunidas for the economic support to finance her scholarship in Residencia de Estudiantes and Spanish Ministry of Education for her FPU grant (FPU17/04333).

Appendix A. Supplementary data

Supplementary data to this article can be found online at https://doi.org/10.1016/j.watres.2020.116074.

References

Castro-Alférez, M., Inmaculada Polo-López, M., Marugán, J., Fernández-Ibáñez, P., 2018. Validation of a solar-thermal water disinfection model for *Escherichia coli* inactivation in pilot scale solar reactors and real conditions. Chem. Eng. J. 331, 831–840. https://doi.org/10.1016/j.cej.2017.09.015.

Castro-Alférez, M., Polo-López, M.I., Marugán, J., Fernández-Ibáñez, P., 2017. Mechanistic modeling of UV and mild-heat synergistic effect on solar water disinfection. Chem. Eng. J. 316, 111–120. https://doi.org/10.1016/j.cej.2017.01.026.

Davies-Colley, R.J., Donnison, A.M., Speed, D.J., 2000. Towards a mechanistic understanding of pond disinfection. Water Sci. Technol. 42, 149–158. https://doi.org/10.2166/wst.2000.0630.

Fisher, M.B., Iriarte, M., Nelson, K.L., 2012. Solar water disinfection (SODIS) of *Escherichia coli, Enterococcus spp.*, and MS2 coliphage: effects of additives and alternative container materials. Water Res. 46, 1745–1754. https://doi.org/10.1016/j.watres.2011.12.048.

Fisher, M.B., Keenan, C.R., Nelson, K.L., Voelker, B.M., 2008. Speeding up solar disinfection (SODIS): effects of hydrogen peroxide, temperature, pH, and copper plus ascorbate on the photoinactivation of *E. coli*. J. Water Health 6, 35–51. https://doi.org/10.2166/wh.2007.005.

Fisher, M.B., Love, D.C., Schuech, R., Nelson, K.L., 2011. Simulated sunlight action spectra for inactivation of MS2 and PRD1 bacteriophages in clear water. Environ. Sci. Technol. 45, 9249–9255. https://doi.org/10.1021/es201875x.

García-Gil, Á., Pablos, C., García-Muñoz, R.A., McGuigan, K.G., Marugán, J., 2020a. Material selection and prediction of solar irradiance in plastic devices for application of solar water disinfection (SODIS) to inactivate viruses, bacteria and protozoa. Sci. Total Environ. 730, 139126. https://doi.org/10.1016/j.scitotenv.2020.139126.

García-Gil, Á., Valverde, R., García-Muñoz, R.A., McGuigan, K.G., Marugán, J., 2020b. Solar Water Disinfection in High-Volume Containers: Are Naturally Occurring Substances Attenuating Factors of Radiation? Chem. Eng. J. 399. https://doi.org/10.1016/j.cej.2020.125852.

Gómez-Couso, H., Fontán-Sainz, M., Ares-Mazás, E., 2010. Thermal contribution to the inactivation of *Cryptosporidium* in plastic bottles during solar water disinfection procedures. Am. J. Trop. Med. Hyg. 82, 35–39. https://doi.org/10.4269/ajtmh.2010.09-0284.

Kohn, T., Grandbois, M., Mcneill, K., Nelson, K.L., 2007. Association with natural organic matter enhances the sunlight-mediated inactivation of MS2 coliphage by singlet oxygen. Environ. Sci. Technol. 41, 4626–4632. https://doi.org/10.1021/es070295h.

Kohn, T., Mattle, M.J., Minella, M., Vione, D., 2016. A modeling approach to estimate the solar disinfection of viral indicator organisms in waste stabilization ponds and surface waters. Water Res. 88, 912–922. https://doi.org/10.1016/

j.watres.2015.11.022.
Kohn, T., Nelson, K.L., 2007. Sunlight-Mediated inactivation of MS2 coliphage *via* exogenous singlet oxygen produced by sensitizers in natural waters. Environ. Sci. Technol. 41, 192–197. https://doi.org/10.1021/ES061716l.
Love, D.C., Silverman, A., Nelson, K.L., 2010. Human virus and bacteriophage inactivation in clear water by simulated sunlight compared to bacteriophage inactivation at a Southern California beach. Environ. Sci. Technol. 44, 6965–6970. https://doi.org/10.1021/es1001924.
Lytle, C.D., Sagripanti, J.-L., 2005. Predicted inactivation of viruses of relevance to biodefense by solar radiation. J. Virol. 79, 14244–14252. https://doi.org/10.1128/JVI.79.22.14244-14252.2005.
Mattle, M.J., Vione, D., Kohn, T., 2015a. Conceptual model and experimental framework to determine the contributions of direct and indirect photoreactions to the solar disinfection of MS2, phiX174, and adenovirus. Environ. Sci. Technol. 49, 334–342. https://doi.org/10.1021/es504764u.
Mattle, M.J., Vione, D., Kohn, T., 2015b. Conceptual model and experimental framework to determine the contributions of direct and indirect photoreactions to the solar disinfection of MS2, phiX174, and adenovirus. Environ. Sci. Technol. 49, 334–342. https://doi.org/10.1021/es504764u.
Maynard, H.E., Ouki, S.K., Williams, S.C., 1999. Tertiary lagoons: a review of removal mechanisms and performance. Water Res. 33, 1–13. https://doi.org/10.1016/S0043-1354(98)00198-5.
McGuigan, K.G., Conroy, R.M., Mosler, H.-J., Preez, M. du, Ubomba-Jaswa, E., Fernandez-Ibañez, P., 2012. Solar water disinfection (SODIS): a review from bench-top to roof-top. J. Hazard Mater. 235, 29–46. https://doi.org/10.1016/j.jhazmat.2012.07.053.
McGuigan, K.G., Joyce, T.M., Conroy, R.M., Gillespie, J.B., Elmore-Meegan, M., 1998. Solar disinfection of drinking water contained in transparent plastic bottles: characterizing the bacterial inactivation process. J. Appl. Microbiol. 84, 1138–1148. https://doi.org/10.1046/j.1365-2672.1998.00455.x.
Nelson, K.L., Boehm, A.B., Davies-Colley, R.J., Dodd, M.C., Kohn, T., Linden, K.G., Liu, Y., Maraccini, P.A., McNeill, K., Mitch, W.A., Nguyen, T.H., Parker, K.M., Rodriguez, R.A., Sassoubre, L.M., Silverman, A.I., Wigginton, K.R., Zepp, R.G., 2018. Sunlight-mediated inactivation of health-relevant microorganisms in water: a review of mechanisms and modeling approaches. Environ. Sci. Process. Impacts 20, 1089–1122. https://doi.org/10.1039/c8em00047f.
Peleg, M., Normand, M.D., Corradini, M.G., 2012. The Arrhenius equation revisited. Crit. Rev. Food Sci. Nutr. 52, 830–851. https://doi.org/10.1080/10408398.2012.667460.
Romero, O.C., Straub, A.P., Kohn, T., Nguyen, T.H., 2011. Role of temperature and Suwannee River Natural Organic Matter on inactivation kinetics of rotavirus and bacteriophage MS2 by solar irradiation. Environ. Sci. Technol. 45, 10385–10393. https://doi.org/10.1021/es202067f.
Rosado-Lausell, S.L., Wang, H., Gutiérrez, L., Romero-Maraccini, O.C., Niu, X.Z., Gin, K.Y.H., Croué, J.P., Nguyen, T.H., 2013. Roles of singlet oxygen and triplet excited state of dissolved organic matter formed by different organic matters in bacteriophage MS2 inactivation. Water Res. 47, 4869–4879. https://doi.org/10.1016/j.watres.2013.05.018.
Silverman, A.I., Tay, N., Machairas, N., 2019. Comparison of biological weighting functions used to model endogenous sunlight inactivation rates of MS2 coliphage. Water Res. 151, 439–446. https://doi.org/10.1016/j.watres.2018.12.015.
Sinton, L.W., Hall, C.H., Lynch, P.A., Davies-Colley, R.J., 2002. Sunlight inactivation of fecal indicator bacteria and bacteriophages from waste stabilization pond effluent in fresh and saline waters. Appl. Environ. Microbiol. 68, 1122–1131. https://doi.org/10.1128/AEM.68.3.1122-1131.2002.
Theitler, D.J., Nasser, A., Gerchman, Y., Kribus, A., Mamane, H., 2012. Synergistic effect of heat and solar UV on DNA damage and water disinfection of *E. Coli* and bacteriophage MS2. J. Water Health 10, 605–618. https://doi.org/10.2166/wh.2012.072.
WHO, 2002. Managing Water in the Home: Accelerated Health Gains from Improved Water Supply.